Stem Cell Reports, Volume *18*

Supplemental Information

Integrated transcriptome-proteome analyses of human stem cells reveal source-dependent differences in their regenerative signature

Abantika Ganguly, Ganesh Swaminathan, Fernando Garcia-Marques, Shobha Regmi, Reza Yarani, Rosita Primavera, Shashank Chetty, Abel Bermudez, Sharon J. Pitteri, and Avnesh S. Thakor

INTEGRATED TRANSCRIPTOME-PROTEOME ANALYSES OF UMBILICAL CORD AND ADULT MESENCHYMAL STEM CELLS REVEAL SOURCE-DEPENDENT DIFFERENCES IN THEIR REGENERATIVE SIGNATURES

Supplementary Methods

Cell Cultutre and Growth Media Conditions

In brief, cells were cultured in a humidified incubator at 5% CO_2 at 37°C using xeno-free and serum-free MesenCult Complete Media (StemCell technologies, USA) and an antibiotic-nutrient solution: Penicillin-Streptomycin-L-glutamine (ThermoFisher, USA), until 70% confluency was reached. This overcomes issues associated with cell culture media variability. Cells were detached using Accutase (Sigma-Aldrich, Switzerland) and pelleted down by centrifugation at 500 g for 5 mins. For all -omics studies, MSCs between P 3-5 were used for data collection. For secretome analysis, cells were changed to fresh MesenCult Media when they reached 60-70% confluency and grown for an additional 48 h prior to the collection of conditioned media (CM). In order to remove cell debris, the CM was centrifuged at 2000 g for 20 mins. Cells were counted using the trypan blue exclusion method.

For the in vitro experiments, murine macrophage/monocyte RAW264.7 and murine encothelial cell line MS-1 was seeded in a monolayer in complete media (DMEM + 10% FBS) (ThermoFisher, United States). For immunogenic and angiogenic assays they media was changed to serum-free basal DMEM when they were 70-80% confluent.

Human Renal Epithelial cell line (HK-2) was grown in Keratinocyte Serum Free Media (Thermofisher, United States) containing 0.05mg/ml Bovine Pituitary extract (BPE) (Sigma-Aldrich, United States) and human recombinant epidermal growth factor (EGF) (Sigma-Aldrich, United States).

Transcriptomics

RNA was extracted using the RNAeasy mini kit (Qiagen,Germany) following the manufacturer's instructions with the RNA quality evaluated by the Agilent Bioanalyzer 2100 system. Only preparations with RNA integrity number (RIN) values ≥ 6.8 were considered. Paired -end 150 bp sequencing was carried out on a Illumina platform.

NGS was performed using the Illumina HiSeq4000 platform. The quality assessment, read filtering and mapping were performed based using NGS QC toolkit and aligned using STAR tool (1) against Human Reference Genome GRCh38. HTSeq was used to quantify the reads (2).

Proteomics Sample Preparation and Analysis

Samples were prepared and analyzed following the protocol described on Rajendran J. C. Bose et al(3). Briefly, cell pellets were lysed with 300 µL of lysis buffer consisting of 2 % sodium dodecyl sulfate (SDS, Fisher Scientific) and 1X protease inhibitor (Sigma-Aldrich). Next, lysed samples were sonicated using a Branson probe sonicator (Fisher Scientific), centrifuged, and proteins were quantified using a bicinchoninic acid (BCA, Thermo Fisher Scientific) protein assay. We used 25 µg of protein for shotgun proteomics. First, the proteins were reduced with Tris(2-carboxyethyl)phosphinehydrochloride (TCEP, Sigma-Aldrich), alkylated with iodoacetamide (Across Organics), and acetone (Fisher Scientific) precipitated overnight at -20°C. The samples were centrifuged at 14,000 g for 10 min at 4 °C and acetone was discarded. Precipitated proteins were digested with 1 µg of sequencing grade modified trypsin (Thermo Fisher Scientific) in 50 µL of 50 mM ammonium bicarbonate (Sigma-Aldrich) at 37 °C overnight without shaking. The resulting tryptic peptides were dried down and reconstituted in 50 µL of 0.1% formic acid in water (Fisher Scientific). 3 µL of the peptide solution was loaded onto a C18 PepMap 100 trap column (Thermo Fisher Scientific) using a Dionex Ultimate Rapid Separation Liquid Chromatography system (Thermo Fisher Scientific) at a flow rate of 5 µL/min for 10 minutes and separated by reversed-phased liquid chromatography on a 25 cm long analytical column (New Objective) packed with Magic C18 AQ resin (Michrom Bioresources) at a constant flow rate of 0.5 µL/min. The chromatography gradient consisted of holding buffer A (0.1 % formic acid in water) at 98% for the first 10 minutes with a slow increase of buffer B (0.1 % formic acid in acetonitrile) to 35% in 100 min, followed by an increased to 85 % B over 7 min with a 5 min hold time. Eluted peptides were analyzed on an LTQ Orbitrap Elite mass spectrometer (Thermo Fisher Scientific). The mass spectrometer was programed to select the top 10 most abundant ions per MS1 scan for higher energy collision induced dissociation (35 eV) in a data-dependent fashion with a mass resolution power of 60,000 in the FT with an AGC target value of 1E6 and a m/z scan range of m/z 400-1800. Dynamic exclusion was enabled for 30 s.

Search parameters included trypsin digestion with ≤ 2 miss cleavages, a fixed carbamidomethylation (+57.021 Da) modification on Cysteines, and a variable modification on methionine (+15.994) and asparagine (+0.984). The MS1 precursor and fragment mass tolerances were set to 10 ppm and 0.5 Da respectively. Peptide identifications were filtered A R script based on MSnbase package (4)

was used for the AUC of the extracted ion current (XIC) of all remaining peptides after alignment of the chromatographic runs. Then protein abundances changes were analyzed using the Generic Integration Algorithm.

To perform the protein and RNA-seq quantitative comparison, we applied the same statistical model to normalize the RNA-seq FPKM into *Z-score* of log2 ratio of each measured condition relative to the average of all conditions measured.

Fig S1

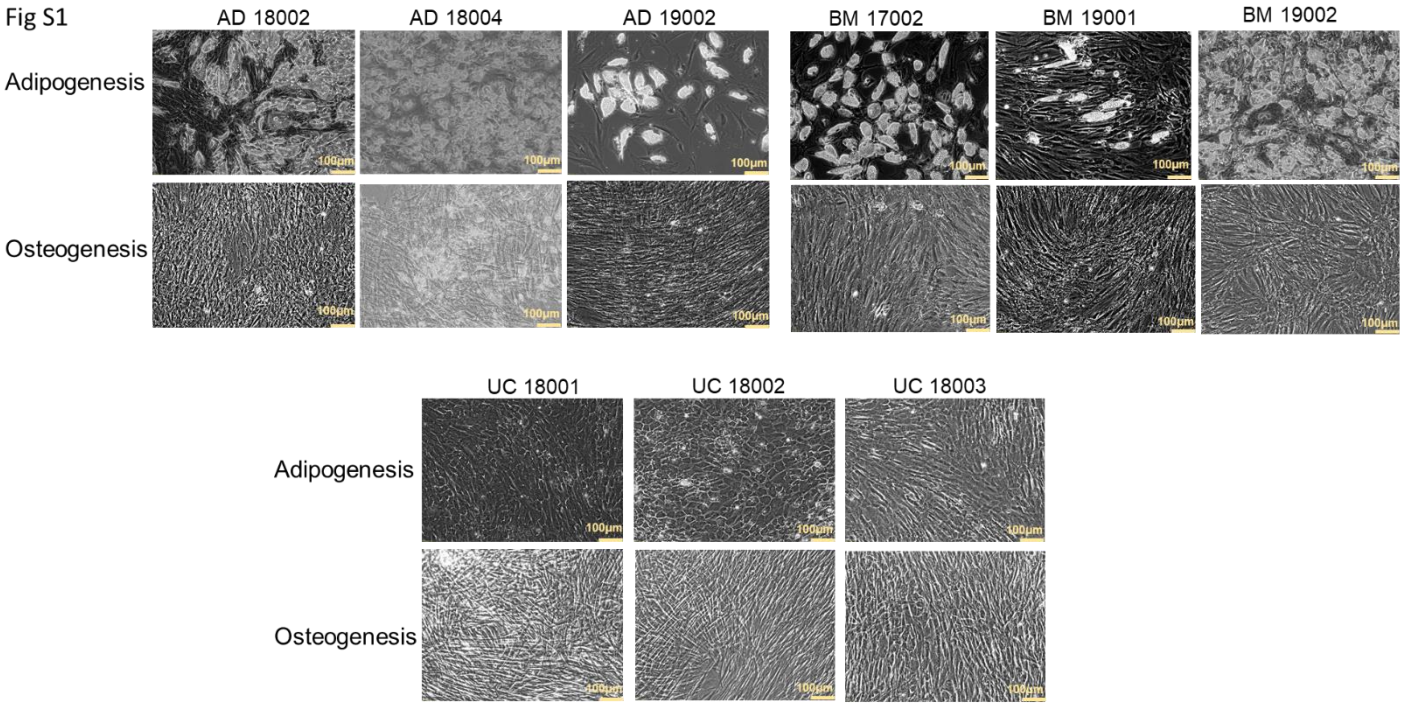

Fig S1: **Cell differentiation characterization of MSCs**. Adipogenic and Osteogenic differentiation ability for each of the 3 donors from AD-MSC, BM-MSC and UC-MSC sources used in this study. Adipogenesis was measured using Oil Red O staining and Osteogenesis was measured using von Kossa staining. Scale bar = 100µm.

Fig S2

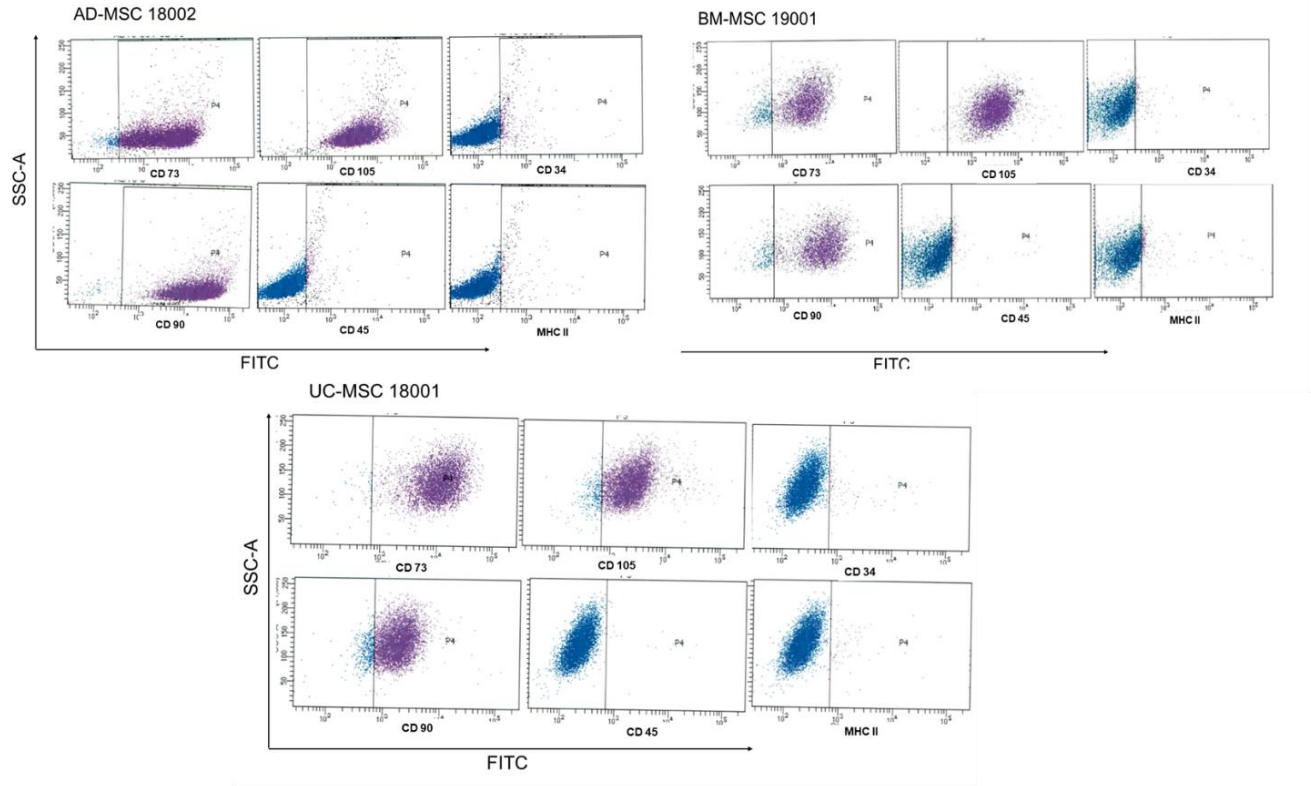

Fig S2: **Phenotypic characterization of MSCs.** Flow cytometry data indicates presence of MSC markers – CD73, CD105 and CD90. It also indicates the absence of hematopoietic markers CD34, CD45 and MHC II in AD-MSC , BM-MSC and UC-MSC used in our study. Data is shown for one representative donor.

Fig S3

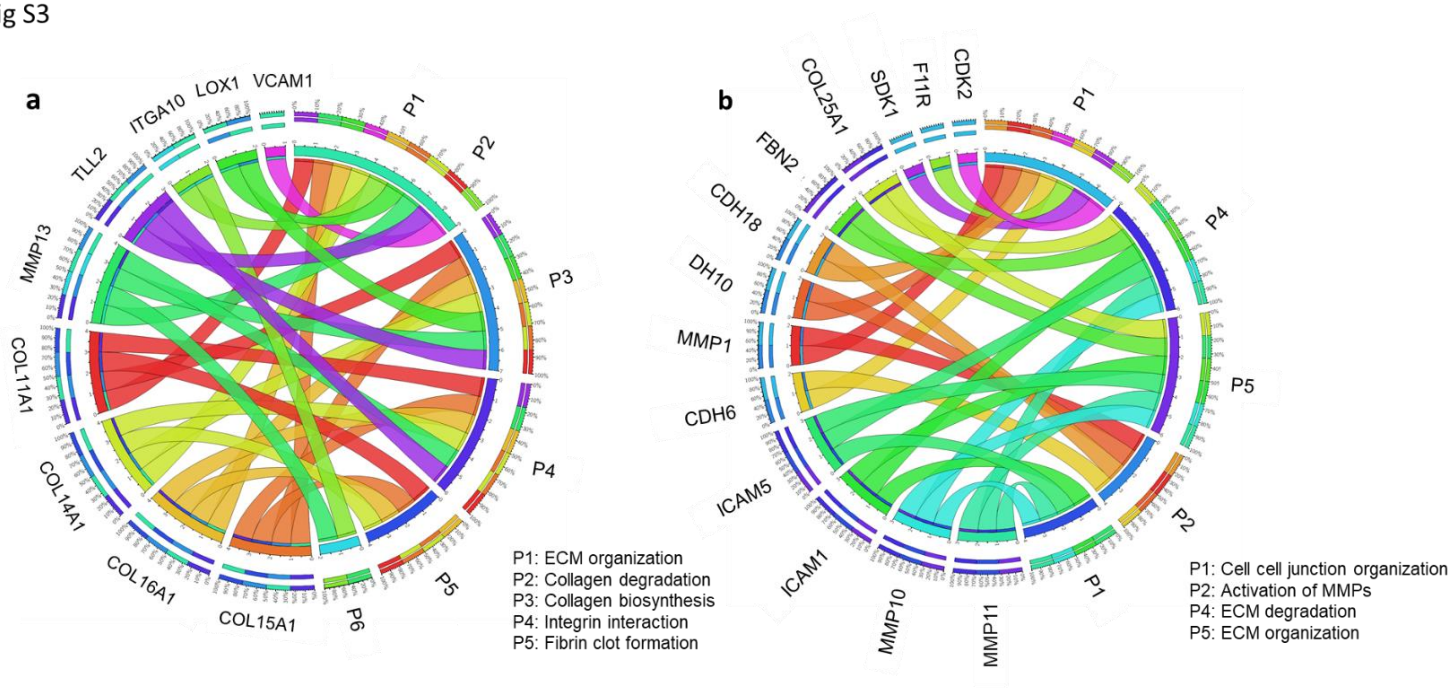

Fig S3: **Comparison of ECM remodeling genes upregulated in UC-MSC vs adult-MSC.** Circos plot demonstrates the relationship between various ECM remodeling pathways and their corresponding genes which were found to be significantly enriched (FDR < 0.05) in (a) UC-MSC and (b) adult-MSC.

Fig S4

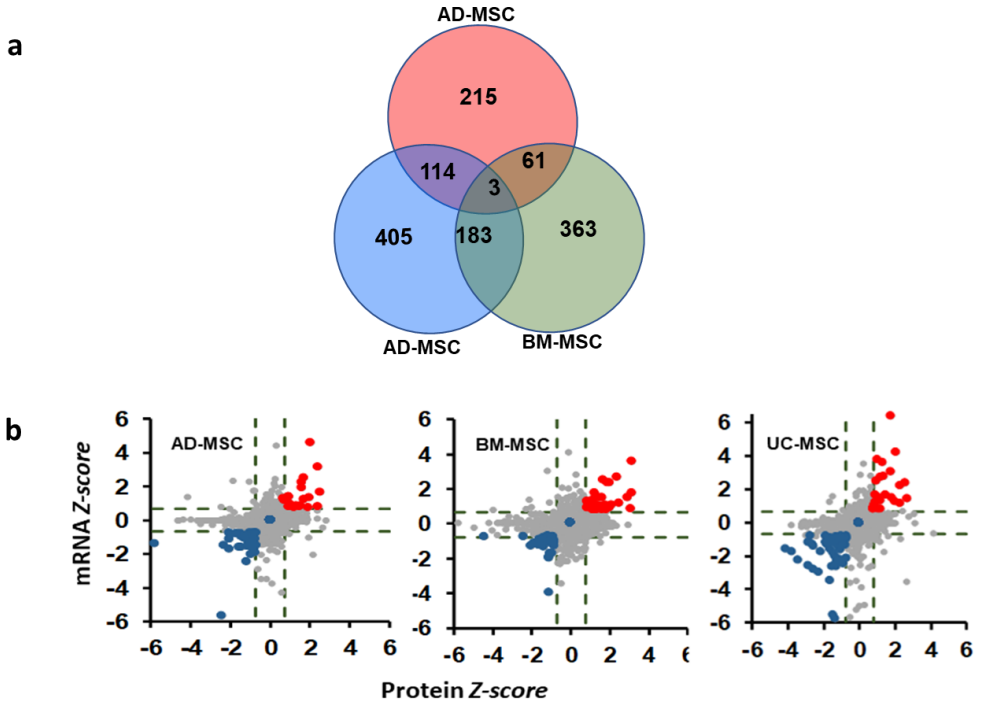

Fig S4: **Proteomics Analysis for three different sources of MSC. (a)** Venn diagram showing the number of statistically significant proteins (FDR < 0.05) enriched in each MSC source and the overlap between them. (b) Correlation coefficient between the mRNA transcripts and proteomics dataset based on their Z-scores. Grey : high correlated genes Red: upregulated genes that were differentially expressed between mRNA and protein datasets. Blue: downregulated genes that were differentially expressed between mRNA and protein datasets.

Fig S5

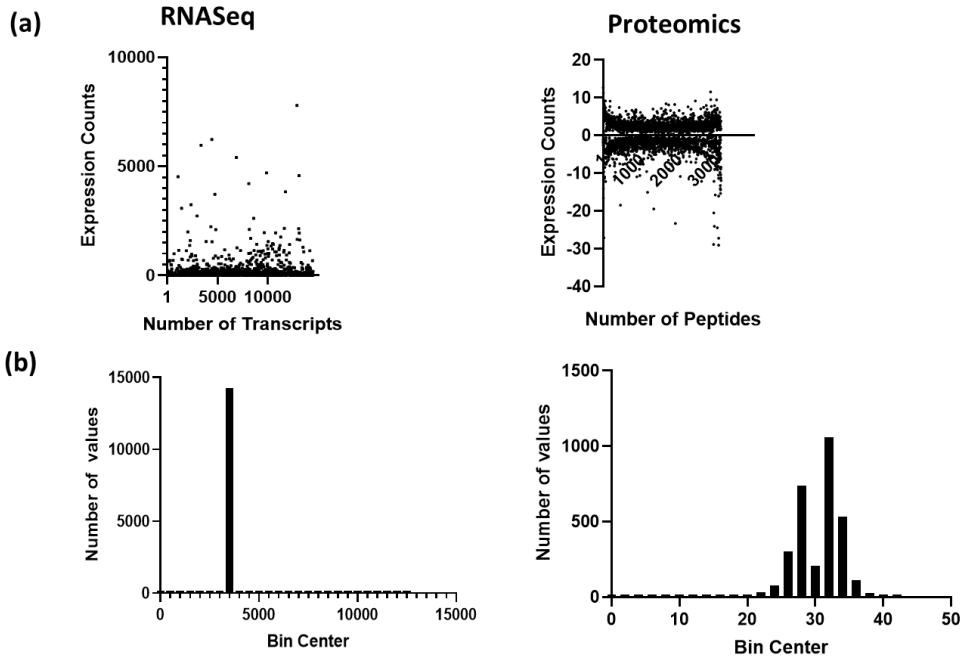

Fig S5 (a) Dispersion of expression values of mRNA transcript and peptides identified from LC/MS dataset. (b) Frequency distribution for the number of targets (transcripts and peptides) associated with a particular BIN value

Fig S6

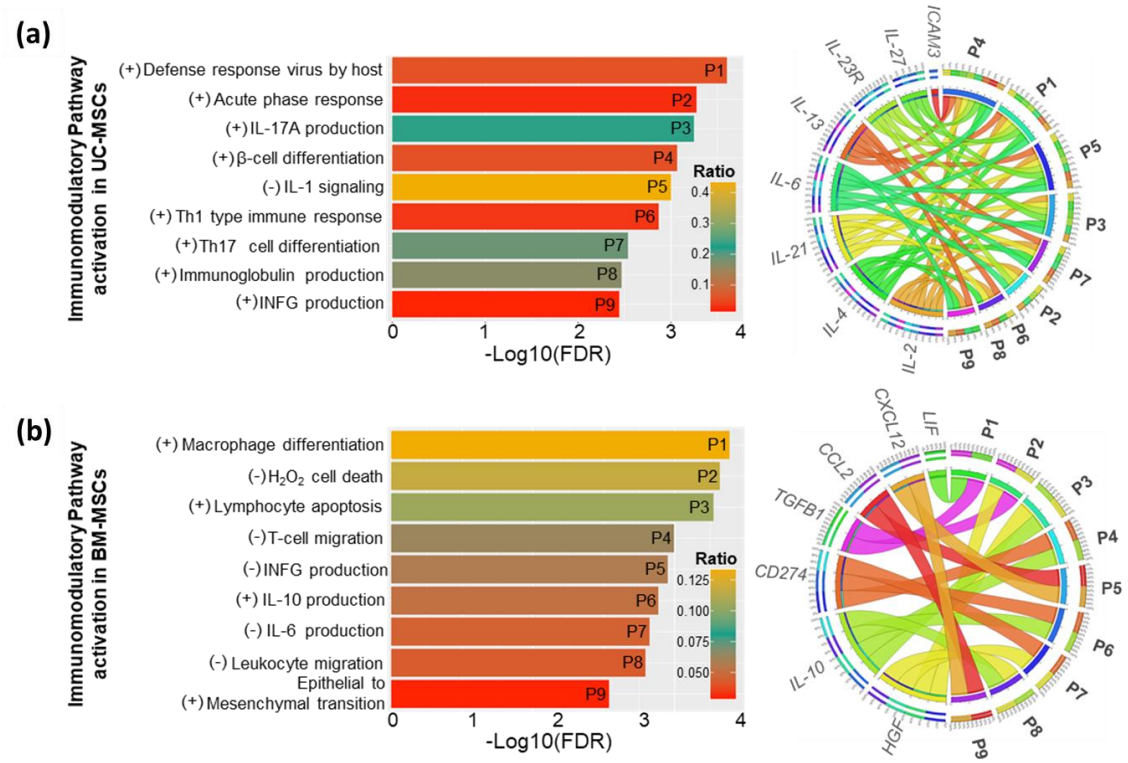

Fig S6 (a) Statistically significant (FDR < 0.05) immune-regulatory pathways enriched in UC-MSC cultured media and Circos plot depicting the relationship between enriched immune-regulatory pathways and their corresponding genes identified in our PPI network. (b) Statistically significant (FDR < 0.05) immune-regulatory pathways enriched in adult-MSC cultured media and Circos plot depicting the relationship between enriched immune-regulatory pathways and their corresponding genes identified in our PPI network.

Fig S7

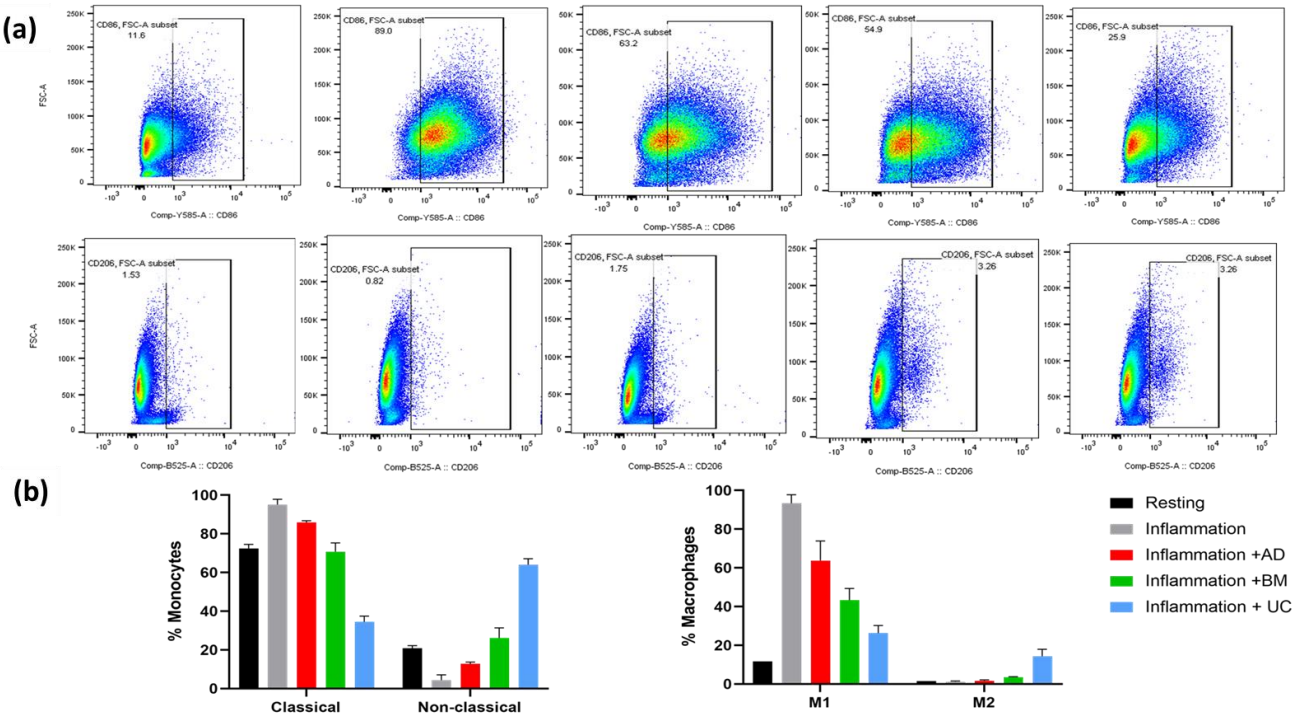

Fig S7 (a) Flow cytometry showing the change in population of CD86 (M1 macrophage) and CD206 (M2 macrophage) following incubation with different sources of MSCs. (b) Plot showing the percentage of classical/non-classical monocytes and M1 and M2 macrophages with different sources of MSCs after activation

Table S1: Human MSC donor details used for this study

Source	Donor Number	Age	Sex	Ethnicity
bone marrow	*17-002*	*23*	*male*	*Hispanic*
bone marrow	*19-001*	*22*	*female*	*African-American*
bone marrow	*19-002*	*21*	*male*	*African-American*
adipose tissue	*18-002*	*37*	*female*	*Caucasian*
adipose tissue	*18-004*	*19*	*male*	*Hispanic*
adipose tissue	*19-002*	*23*	*male*	*Caucasian*
umbilical cord-Wharton's jelly	*18-001*	*NA*	*NA*	*NA*
umbilical cord-Wharton's jelly	*18-002*	*NA*	*NA*	*NA*
umbilical cord-Wharton's jelly	*18-003*	*NA*	*NA*	*NA*

Table S2: human MSC donor Phenotypic Characterization

Donor	Age	Sex	Ethnicity	Viability (Trypan Blue)	Adipogenesis (Oil Red O Staining)	Osteogenesis (Von Kossa Staining)
AD 18002	37	F	Caucasian	> 70%	+	+
AD 18004	19	M	Hispanic	> 70%	+	+
AD 19002	23	M	Caucasian	> 70%	+	+
BM17002	23	M	Hispanic	> 70%	+	+
BM 19002	21	M	African-American	> 70%	+	+
BM 19001	22	F	African American	> 70%	+	+
UC 18001	NA	NA	-	> 70%	+	+
UC 18002	NA	NA	-	> 70%	+	+
UC 19002	NA	NA	-	> 70%	+	+

Table S3: Functional properties of human MSC secretome array

Category	Function	Secretory Factors
Pro-Angiogenic Factors		
Growth Factors	angiogenesis and proliferation	*SCF; EGF; FGF-2/FGF-b; PDGF-AA; PDGF-AB/BB; TGF-a; VEGF-A; HGF; CX3CL1; CXCL5; CXCL8; CXCL12; sVCAM-1*
Pro-angiogenic immune mediators	differentiation and proliferation of immune cells	*CCL26; CXCL12; CCL22; CCL17; LIF; IFNA2; IL-1Ra; IL-4; IL-10; IL-13; IL-6; IL-23; IL-2; IL-22; IL-21; IL-27; IL-17E; G-CSF; sICAM1*
Immunomodulatory Factors		
Anti-inflammatory	Inhibit proliferation of T-cells but may promote Th1 cell differentiation	*CXCL13; CX3CL1; CXCL5; CXCL8; CXCL1; CXCL10; CXCL9; M-CSF; GM-CSF; CCL8; CCL13; CCL1; CCL27; CCL15; CCL11; CCL3; CCL21; CCL24; CCL27; CCL5; IL-1a; IL-1b*
Immunosuppressive	Promotes Th2 and Tregs differentiation to maintain Th1/Th2 balance. Inhibits Th17 pathway	*sVCAM-1; G-CSF; CCL22; CCL17; CCL2; LIF; IL-3; IL-10; IL-4; TGF-a; CXCL12; HGF*

Data S4: mRNA transcriptomics -FPKM and DEG values; GO pathway analysis

Data S5: raw read count and Z-score for proteomics; GO pathway analysis

Data S6: Z-score for transcriptomics and proteomics comparison, DEP, Reactome Pathway Analysis

Data S7: Secretome_MFI : raw and normalized counts

1. Dobin A, Davis CA, Schlesinger F, Drenkow J, Zaleski C, Jha S, Batut P, Chaisson M, Gingeras TR. STAR: ultrafast universal RNA-seq aligner. Bioinformatics (Oxford, England). 2013;29(1):15-21. Epub 2012/10/30. doi: 10.1093/bioinformatics/bts635. PubMed PMID: 23104886; PMCID: PMC3530905.
2. Anders S, Pyl PT, Huber W. HTSeq--a Python framework to work with high-throughput sequencing data. Bioinformatics (Oxford, England). 2015;31(2):166-9. Epub 2014/09/25. doi: 10.1093/bioinformatics/btu638. PubMed PMID: 25260700.
3. Bose RJC, Tharmalingam N, Garcia Marques FJ, Sukumar UK, Natarajan A, Zeng Y, Robinson E, Bermudez A, Chang E, Habte F, Pitteri SJ, McCarthy JR, Gambhir SS, Massoud TF, Mylonakis E, Paulmurugan

R. Reconstructed Apoptotic Bodies as Targeted “Nano Decoys” to Treat Intracellular Bacterial Infections within Macrophages and Cancer Cells. ACS Nano. 2020;14(5):5818-35. doi: 10.1021/acsnano.0c00921.
4. Gatto L, Lilley KS. MSnbase-an R/Bioconductor package for isobaric tagged mass spectrometry data visualization, processing and quantitation. Bioinformatics (Oxford, England). 2012;28(2):288-9. Epub 2011/11/25. doi: 10.1093/bioinformatics/btr645. PubMed PMID: 22113085.